SUPPLEMENTAL FIGURES

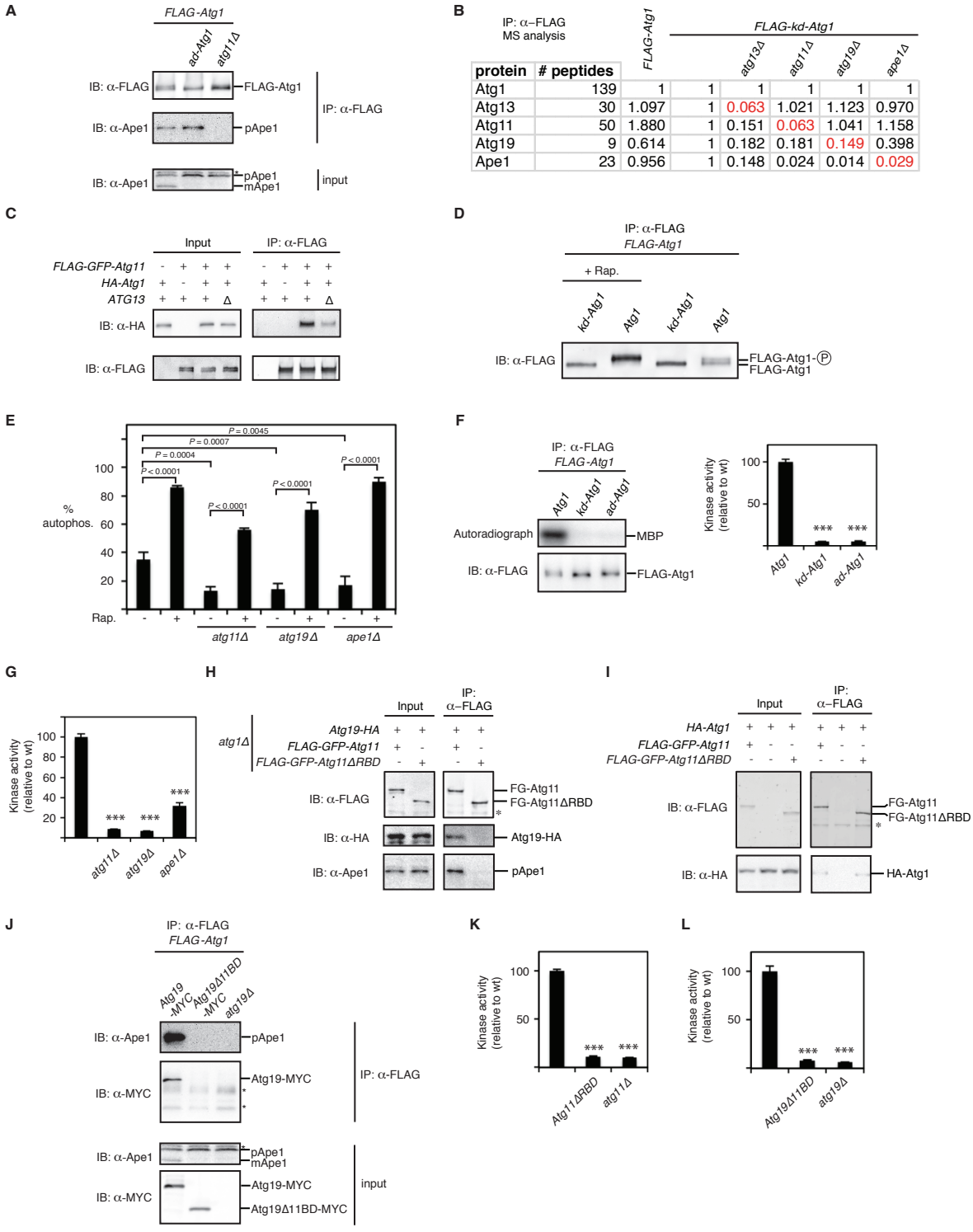

Figure S1. Analysis of protein-protein interactions between Atg1 complex subunits, related to Figure 1.

(**A**) Extracts derived from logarithmically growing cells with indicated genotypes were immunoprecipitated (IP) with anti-FLAG magnetic beads as in Figure 1B. Eluates and extract (input) samples were resolved by SDS-PAGE followed by immunoblotting (IB) with the indicated antibodies. *, non-specific band.

(**B**) Extracts derived from logarithmically growing cells with indicated genotypes were immunoprecipitated with anti-FLAG magnetic beads. Eluates were analyzed by quantitative mass spectrometry (MS) (see Supplemental Experimental Procedures for details). Shown is the number (#) of unique tryptic peptides used to quantify each protein abundance. After normalizing the levels of FLAG-Atg1 to correct for input differences between samples, relative abundance of each protein was compared to the amount associated with FLAG-*kd*-Atg1, which was set to 1. Highlighted in red is the nominal abundance of proteins that were in fact absent from those samples.

(**C**) Extracts derived from logarithmically growing cells with indicated genotypes (minus indicates absence of corresponding epitope tag; Δ indicates *atg13Δ*) were immunoprecipitated (IP) with anti-FLAG magnetic beads. Eluates and extract (input) samples were resolved by SDS-PAGE followed by immunoblotting (IB) with the indicated antibodies.

(**D**) Logarithmically growing cells with indicated genotypes were treated with rapamycin (Rap.) or mock treated prior to immunoprecipitation (IP) analysis as in Figure 1B with one notable exception: SDS-PAGE was done for a longer time to resolve Atg1 from its autophosphorylated form (Atg1-P), as visualized by immunoblotting (IB). *kd,* kinase-dead allele.

(**E**) Statistical analysis of data from Figure 1D. Plotted data represent mean +/- standard deviation (error bars) for each sample (n=3). Indicated p values are derived from Tukey's post-test. $p < 0.01$ was considered significant.

(**F**) Myelin basic protein (MBP) phosphorylation by FLAG-Atg1 immunoprecipitated (IP) from indicated extracts was carried out as in Figures 1E-G. *kd,* kinase-dead allele; *ad,* autoactivation-dead allele. Statistical analysis is shown on right. Plotted data represent mean +/- standard deviation (error bars) for each sample (n=3). p values derived from Tukey's post-test are reported only for comparisons between each mutant and the wild-type reaction. ***$p < 0.0001$.

(**G**) Statistical analysis of data from Figure 1E. Plotted data represent mean +/- standard deviation (error bars) for each reaction (n=3). p values derived from Tukey's post-test are reported only for comparisons between each mutant and the wild-type reaction. ***$p < 0.0001$.

(**H** and **I**) Extracts derived from logarithmically growing cells with indicated genotypes (minus indicates absence of corresponding epitope tag) were immunoprecipitated (IP) with anti-FLAG magnetic beads. Eluates and extract (input) samples were resolved by SDS-PAGE followed by immunoblotting (IB) with the indicated antibodies. *, non-specific band.

(**J**) The exact same eluates and extract (input) samples shown in Figure 1G were resolved by SDS-PAGE followed by immunoblotting (IB) with indicated antibodies. For simplicity, we did

not indicate MYC-tagging of Atg19 in Figure 1G and we refer the reader to that figure for IP/IB anti-FLAG data that control for any loading differences. *, non-specific band.

(**K**) Statistical analysis of data from Figure 1F. Plotted data represent mean +/- standard deviation (error bars) for each reaction (n=3). p values derived from Tukey's post-test are reported only for comparisons between each mutant and the wild-type reaction. ***$p < 0.0001$.

(**L**) Statistical analysis of data from Figure 1G. Plotted data represent mean +/- standard deviation (error bars) for each reaction (n=3). p values derived from Tukey's post-test are reported only for comparisons between each mutant and the wild-type reaction. ***$p < 0.0001$.

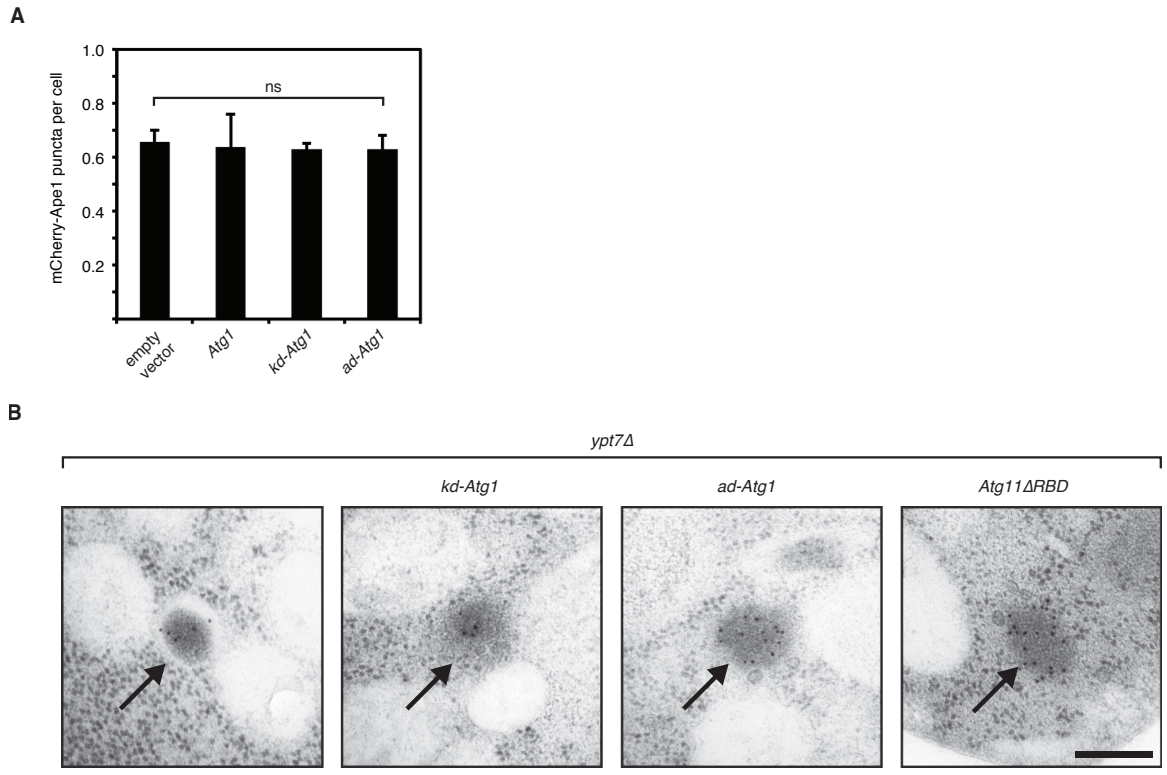

Figure S2. Atg1 kinase activity and autoactivation are required for selective autophagosome membrane expansion in nourished cells, related to Figure 2.

(**A**) Image analysis of strains shown in Figure 2A. Bar graphs report the number of mCherry-Ape1 puncta per cell as the mean and standard deviation (error bars) from three independent experiments (>1500 cells per strain per experiment analyzed). There were no statistically significant differences at the $p < 0.05$ level as determined by one-way ANOVA. ns, not significant.

(**B**) Additional representative transmission electron micrographs of logarithmically growing *ypt7*Δ cells expressing the indicated mutant alleles from their endogenous genomic loci. Black arrows indicate immunogold-labeled Ape1 aggregates. Scale bar, 200 nm.

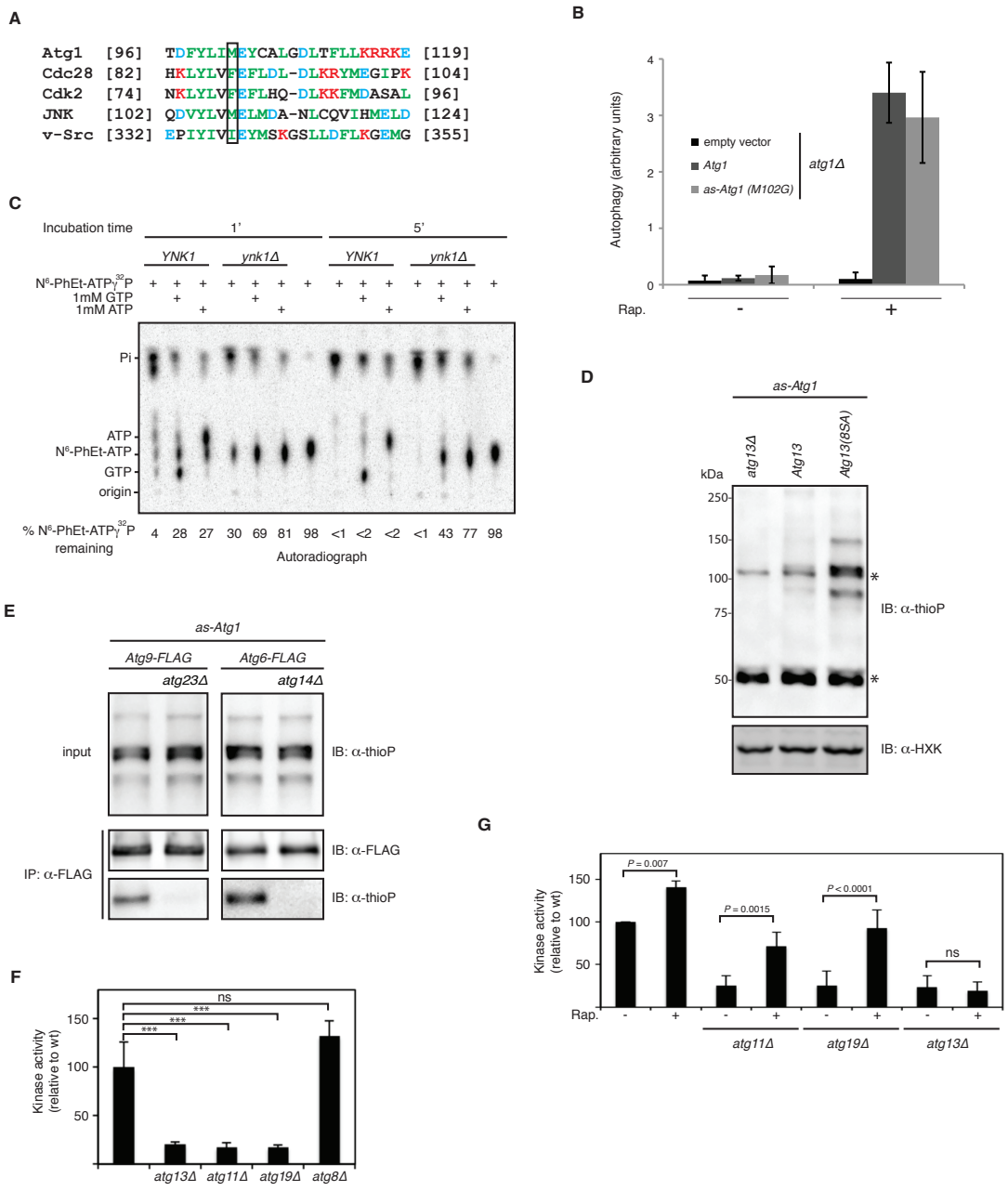

Figure S3. Development of a cell-free assay for Atg1 kinase activity, related to Figure 3.

(**A**) Sequence alignment of Atg1's "gatekeeper" residue (M102, boxed) with that of previously modified kinases. Red, basic residues; Blue, acidic residues; Green, hydrophobic residues.

(**B**) Logarithmically growing *atg1*Δ cells carrying the indicated vectors were treated with rapamycin (Rap.) or mock-treated followed by analysis of an alkaline phosphatase reporter of non-selective autophagy (see Supplemental Experimental Procedures for details). Bar graphs report the mean (n=3) and standard deviation (error bars) of alkaline phosphatase activity in arbitrary units.

(**C**) Radiolabelled N^6-PhEt-ATPγ^{32}P was incubated for the indicated times in *YNK1* and *ynk1*Δ cell extracts (*n.b.* both extracts have wild-type Atg1) supplemented with indicated nucleotides. Samples were resolved by thin layer chromatography and visualized by autoradiography. N^6-PhEt-ATPγ^{32}P signal from autoradiograph was quantified by densitometry and is reported below the plate image as a percentage of the starting amount.

(**D**) Total *as*-Atg1 kinase activity of the indicated extracts was measured as described in Figure 3 using gel system 2. HXK, hexokinase; *, non-specific bands.

(**E**) Thiophosphorylation by *as*-Atg1 was measured in the total (input) and immunoprecipitated (IP) fractions of the indicated extracts as described in Figure 3C. Atg23 is required for Atg9 incorporation into post-Golgi vesicles capable of recruitment to the site of autophagosome formation in the cell (Backues et al., 2014). Atg6 is part of a multi-subunit complex that includes Atg14, a subunit necessary for complex recruitment to the site of autophagosome formation in the cell (Obara et al., 2006).

(**F**) Statistical analysis of data from Figure 3D. Signal from anti-thiophosphate ester (thioP) antibody immunoblots was quantified by densitometry relative to the wild-type reaction set at 100. Plotted data represents mean +/- standard deviation (error bars) for each sample (n=3). Pairwise p values were derived from Tukey's post-test. $p < 0.01$ was considered significant. ***$p < 0.0001$; ns, not significant.

(**G**) Statistical analysis of data from Figure 3E comparing the effect of rapamycin on Atg1 kinase activity in different backgrounds. Signal from anti-thiophosphate ester (thioP) antibody immunoblots was quantified by densitometry relative to the wild-type reaction set at 100. Plotted data represents mean +/- standard deviation (error bars) for each sample (n=4). Pairwise p values were derived from Tukey's post-test and p values for relevant comparisons are shown. $p < 0.01$ was considered significant. ns, not significant.

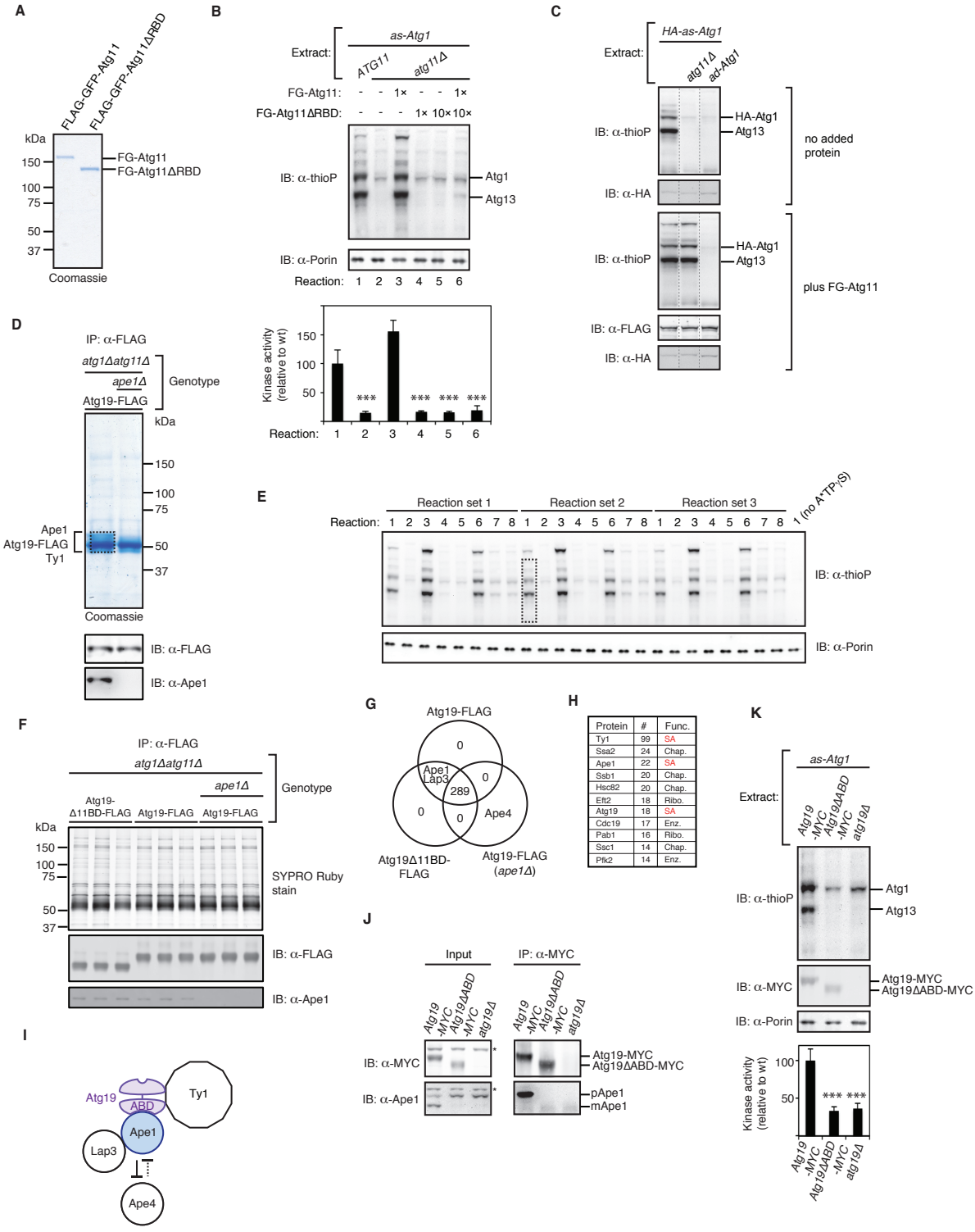

Figure S4. Characterization of affinity-purified Atg11 and Atg19, related to Figure 4.

(**A**) Purified FLAG-GFP-Atg11 and FLAG-GFP-Atg11ΔRBD (see Supplemental Experimental Procedures for details) were analyzed by SDS-PAGE followed by Coomassie staining.

(**B**) *as*-Atg1 kinase analysis of the indicated extracts was carried out in triplicate (one set of reactions is shown) as in Figure 4A, followed by quantification of kinase activity by densitometry. Plotted data represents mean kinase activity (relative to reaction 1, set to 100) +/- standard deviation (error bars) for each reaction (n=3). Immunoblotting (IB) with anti-porin (a mitochondrial protein) was used to control for any gel-loading differences. p values derived from Tukey's post-test for the comparisons between indicated reactions and reaction 1 are shown. ***$p < 0.0001$.

(**C**) HA-*as*-Atg1 extract was pre-incubated with either purified FLAG-GFP-Atg11 (bottom) or mock pre-incubated (top) prior to Atg1 kinase analysis as in Figure 4A. Immunoblotting with indicated antibodies was used to control for protein add-back and any gel-loading differences. Dotted lines indicated that all lanes were spliced from the same gel.

(**D**) Atg19-FLAG was purified from the indicated extracts (see Supplemental Experimental Procedures for details) and analyzed by SDS-PAGE followed by either Coomassie staining or immunoblotting (IB) with indicated antibodies. Proteins listed to left of Coomassie-stained gel indicate the three most abundant proteins detected by mass spectrometry of material in the indicated gel slice (dotted box).

(**E**) Source data for Figure 4D. Dotted box indicates region of gel that was used for densitometric quantification (*n.b.* this region excludes the highest molecular weight band because it corresponds to FG-Atg11, which is being added back to certain reactions). Reaction loaded in rightmost lane was incubated without A*TPγS and used to subtract background signal from *bona fide* phosphorylation. Immunoblotting with anti-porin was used to control for any gel-loading differences.

(**F**) Atg19-FLAG or mutant thereof lacking the Atg11 binding domain (11BD) was purified in triplicate from the indicated extracts (see Supplemental Experimental Procedures) and resolved by SDS-PAGE, followed by SYPRO staining and immunoblotting with the indicated antibodies.

(**G**) Summary of quantitative mass spectrometry analysis of purified complexes shown in part (F). Proteins whose abundance was significantly different between preparations are indicated. For example, Ape1 is present in both Atg19-FLAG and Atg19Δ11BD-FLAG preparations but its absence from cells apparently enables more Ape4 (a distinct aminopeptidase) to interact with Atg19-FLAG. 289 refers to the number of proteins that were identified in all 3 preparations.

(**H**) List of most abundant proteins in each preparation, ranked by number (#) of quantified peptides, with short description of known function (Func.): SA, selective autophagy; Chap., chaperone; Ribo., ribosome-associated protein; Enz., metabolic enzyme.

(**I**) Model of subunit associations within the Atg19 complex based on data from mass spectrometry analysis of eluates shown in (F). Bar arrows indicate apparent competition between Ape1 and Ape4 for binding to Atg19. ABD, Ape1-Binding Domain.

(**J**) Extracts derived from logarithmically-growing cells with indicated genotypes were immunoprecipitated (IP) with anti-MYC magnetic beads. Eluates and extract (input) samples were resolved by SDS-PAGE followed by immunoblotting (IB) with indicated antibodies. *, non-specific band.

(**K**) The indicated *as-ATG1* extracts were analyzed in triplicate for Atg1 kinase activity as in Figure 4A. Statistical analysis shown below. Plotted data represent mean +/- standard deviation (error bars) for each reaction (n=3). Pairwise comparisons derived from Tukey's post-test are reported only for comparisons with Atg19-MYC extract. ***$p < 0.0001$.

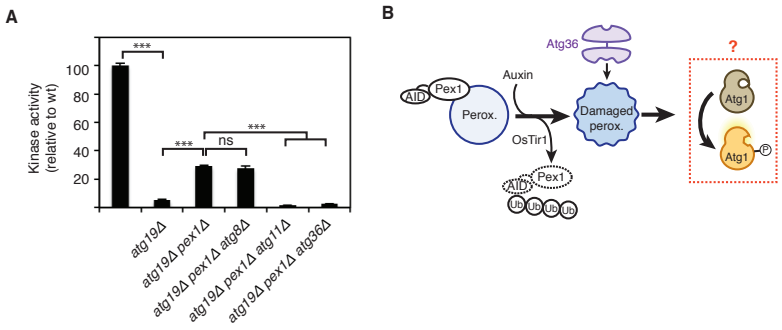

Figure S5. Atg1 activation by damaged peroxisomes, related to Figure 5.

(**A**) Statistical analysis of data from Figure 5A. Plotted data represent mean +/- standard deviation (error bars) for each reaction (n=3). p values derived from Tukey's post-test for a subset of pairwise comparisons are shown. ***$p < 0.0001$; ns, not significant.

(**B**) Schematic showing induction of pexophagy by engineered proteolysis of Pex1. Addition of auxin to cells that express the ubiquitin ligase OsTir1 induces degradation of Pex1-AID (auxin-inducible degron), leading to an undefined damage signal. Presence of Atg36 on damaged peroxisomes enables peroxisome degradation by autophagy, possibly by activating Atg1 (dotted red box). Perox., peroxisome; Ub, ubiquitin.

SUPPLEMENTAL TABLE

Table S1. Yeast strains

Strains	Genotype	Experiment
BY4741	*MATa ura3Δ0 his3Δ1 leu2Δ0 met15Δ0*	background, S1C, S3C
VDY630	*BY4741 atg1Δ::2×-FLAG-ATG1*	1B, 1D, 1F, S1A, S1B, S1D, S1F
VDY2409	*BY4741 atg1Δ::2×-FLAG-ATG1(D211A)*	1B, S1B, S1D, S1F
VDY2416	*BY4741 atg1Δ::2×-FLAG-ATG1(D211A) atg13Δ::LEU*	1B, S1B
VDY2411	*BY4741 atg1Δ::2×-FLAG-ATG1(D211A) atg11Δ::LEU*	1B, S1B
VDY2412	*BY4741 atg1Δ::2×-FLAG-ATG1(D211A) atg19Δ::LEU*	1B, S1B
VDY2413	*BY4741 atg1Δ::2×-FLAG-ATG1(D211A) ape1Δ::LEU*	1B, S1B
VDY2390	*BY4741 atg1Δ::2×-FLAG-ATG1 ape1Δ::LEU*	1D
VDY2387	*BY4741 atg1Δ::2×-FLAG-ATG1 atg11Δ::LEU*	1D, 1F, S1A
VDY2388	*BY4741 atg1Δ::2×-FLAG-ATG1 atg19Δ::LEU*	1D, 1G, S1J
VDY635	*BY4741 atg1Δ::2×-FLAG-ATG1 ynk1Δ::KANMX*	1E
VDY2249	*BY4741 atg1Δ::2×-FLAG-ATG1 ynk1Δ::KANMX atg11Δ::LEU*	1E
VDY2250	*BY4741 atg1Δ::2×-FLAG-ATG1 ynk1Δ::KANMX atg19Δ::URA*	1E
VDY2419	*BY4741 atg1Δ::2×-FLAG-ATG1 ynk1Δ::KANMX ape1Δ::URA*	1E
VDY2527	*BY4741 atg1Δ::2×-FLAG-ATG1 ATG11ΔRBD::NAT*	1F
VDY2576	*BY4741 atg1Δ::2×-FLAG-ATG1 ATG19-13×-MYC::HIS*	1G, S1J
VDY2577	*BY4741 atg1Δ::2×-FLAG-ATG1 ATG19Δ11BD-13×-MYC::HIS*	1G, S1J
VDY2585	*BY4741 atg1Δ::HIS atg17::LEU ape1Δ::mCHERRY-APE1 ATG2-3×-GFP::NAT [pRS316]*	2A, 2B, S2A
VDY2596	*BY4741 atg1Δ::HIS atg17::LEU ape1Δ::mCHERRY-APE1 ATG2-3×-GFP::NAT [pVD395]*	2A, 2B, S2A
VDY2597	*BY4741 atg1Δ::HIS atg17::LEU ape1Δ::mCHERRY-APE1 ATG2-3×-GFP::NAT [pVD546]*	2A, 2B, S2A
VDY2598	*BY4741 atg1Δ::HIS atg17::LEU ape1Δ::mCHERRY-APE1 ATG2-3×-GFP::NAT [pVD594]*	2A, 2B, S2A
VDY2552	*BY4741 atg1Δ::2×-FLAG-ATG1 ypt7Δ::URA*	2C, S2B
VDY2553	*BY4741 atg1Δ::2×-FLAG-ATG1(D211A) ypt7Δ::URA*	2C, S2B
VDY2554	*BY4741 atg1Δ::2×-FLAG-ATG1(T226A) ypt7Δ::URA*	2C, S2B
VDY2555	*BY4741 atg1Δ::2×-FLAG-ATG1 ATG11ΔRBD::NAT ypt7Δ::URA*	2C, S2B
VDY641	*BY4741 ynk1Δ::KANMX atg13Δ::ATG13-8SA*	3B
VDY650	*BY4741 atg1Δ::2×-FLAG-ATG1(M102G) ynk1Δ::KANMX atg13Δ::ATG13-8SA*	3B
VDY732	*BY4741 atg1Δ::ATG1(M102G) ynk1Δ::KANMX atg13Δ::3×-FLAG-ATG13-8SA*	3B
VDY639	*BY4741 atg1Δ::ATG1(M102G) ynk1Δ::KANMX atg13Δ::ATG13-8SA*	3B, S3D
VDY949	*BY4741 ynk1Δ::KANMX atg13Δ::ATG13-8SA ATG2-3×-FLAG::NAT*	3C
VDY725	*BY4741 atg1Δ::ATG1(M102G) ynk1Δ::KANMX atg13Δ::ATG13-8SA ATG2-3×-FLAG::NAT*	3C
VDY951	*BY4741 ynk1Δ::KANMX atg13Δ::ATG13-8SA ATG9-3×-FLAG::NAT*	3C
VDY950	*BY4741 ynk1Δ::KANMX atg13Δ::ATG13-8SA ATG6-3×-FLAG::NAT*	3C
VDY727	*BY4741 atg1Δ::ATG1(M102G) ynk1Δ::KANMX atg13Δ::ATG13-8SA ATG9-3×-FLAG::NAT*	3C, S3E
VDY908	*BY4741 atg1Δ::ATG1(M102G) ynk1Δ::KANMX atg13Δ::ATG13-8SA ATG6-3×-FLAG::NAT*	3C, S3E
VDY2539	*BY4741 atg1Δ::2×-FLAG-ATG1(M102G) ynk1Δ::KANMX atg13Δ::ATG13-8SA atg8Δ::LEU*	3D
VDY649	*BY4741 atg1Δ::2×-FLAG-ATG1 ynk1Δ::KANMX atg13Δ::ATG13-8SA*	3D
VDY2147	*BY4741 atg1Δ::2×-FLAG-ATG1(M102G) ynk1Δ::KANMX atg13Δ::ATG13-8SA*	3D, 3E
VDY773	*BY4741 atg1Δ::2×-FLAG-ATG1(M102G) ynk1Δ::KANMX atg13Δ::ATG13-8SA atg11Δ::NAT*	3D, 3E
VDY1653	*BY4741 atg1Δ::2×-FLAG-ATG1(M102G) ynk1Δ::KANMX atg13Δ::ATG13-8SA atg19Δ:NAT*	3D, 3E

VDY646	*BY4741 atg1Δ::2×-FLAG-ATG1(M102G) ynk1Δ::KANMX atg13Δ::URA*	3D, 3E
VDY666	*BY4741 atg1Δ::ATG1(M102G) ynk1Δ::KANMX atg13Δ::ATG13-8SA atg11Δ::NAT*	4A, 4B, 4C, 4D, S4B, S4E
VDY798	*BY4741 atg1Δ::ATG1(M102G) ynk1Δ::KANMX atg13Δ::ATG13-8SA atg11Δ::6×-FLAG-GFP-ATG11*	4A, 4B, 4C, 4D, S4B, S4E
VDY1794	*BY4741 atg1Δ::ATG1(M102G) ynk1Δ::KANMX atg13Δ::ATG13-8SA atg11Δ::NAT atg19Δ::URA*	4A, 4C, 4D, S4E
VDY2334	*BY4741 atg1Δ::2×-FLAG-ATG1 ynk1Δ::KANMX atg18Δ::LEU*	5A
VDY2529	*BY4741 atg1Δ::2×-FLAG-ATG1 ynk1Δ::KANMX atg18Δ::LEU atg19Δ::URA*	5A
VDY2538	*BY4741 atg1Δ::2×-FLAG-ATG1 ynk1Δ::KANMX atg18Δ::LEU atg19Δ::URA pex1Δ::NAT*	5A
VDY2573	*BY4741 atg1Δ::2×-FLAG-ATG1 ynk1Δ::KANMX atg18Δ::LEU atg19Δ::URA pex1Δ::NAT atg8Δ::HIS*	5A
VDY2574	*BY4741 atg1Δ::2×-FLAG-ATG1 ynk1Δ::KANMX atg18Δ::LEU atg19Δ::URA pex1Δ::NAT atg11Δ::HIS*	5A
VDY2575	*BY4741 atg1Δ::2×-FLAG-ATG1 ynk1Δ::KANMX atg18Δ::LEU atg19Δ::URA pex1Δ::NAT atg36::HIS*	5A
VDY2370	*BY4741 atg1Δ::2×-HA-ATG1(M102G) ynk1Δ::KANMX atg13Δ::ATG13-8SA atg19Δ::URA atg36Δ::LEU*	5B
VDY2379	*BY4741 atg1Δ::NAT atg19Δ::HIS leu2Δ::pGPD-OsTIR1::LEU PEX1-3×-V5-AID::KANMX*	5B
VDY2380	*BY4741 atg1Δ::NAT atg19Δ::HIS leu2Δ::pGPD-OsTIR1::LEU PEX1-3×-V5-AID::KANMX atg36Δ::URA*	5B
VDY2540	*BY4741 atg1Δ::2×-FLAG-ATG1(T226A)*	S1A, S1F
VDY929	*BY4741 atg11Δ::6×-FLAG-GFP-ATG11*	S1C
VDY2584	*BY4741 atg11Δ::6×-FLAG-GFP-ATG11 atg13Δ::LEU*	S1C
VDY2423	*BY4741 atg1Δ::URA ynk1Δ::KANMX atg13Δ::ATG13-8SA atg11Δ::6×-FLAG-GFP-ATG11 ATG19-3×-HA::HIS*	S1H
VDY2424	*BY4741 atg1Δ::URA ynk1Δ::KANMX atg13Δ::ATG13-8SA atg11Δ::6×-FLAG-GFP-ATG11ΔRBD::NAT ATG19-3×-HA::HIS*	S1H
VDY1341	*BY4741 atg1Δ::2×-HA-ATG1(M102G) ynk1Δ::KANMX atg13Δ::ATG13-8SA atg11Δ::6×-FLAG-GFP-ATG11*	S1I
VDY1342	*BY4741 atg1Δ::2×-HA-ATG1(M102G) ynk1Δ::KANMX atg13Δ::ATG13-8SA atg11Δ::6×-FLAG-GFP-ATG11ΔRBD::NAT*	S1I
VDY1413	*BY4741 atg1Δ::2×-HA-ATG1(M102G) ynk1Δ::KANMX atg13Δ::ATG13-8SA*	S1I, S4C
VDY564	*BY4741 pho13Δ::MET KANMX::pTDH3-Pho8Δ1-60 atg1Δ::NAT*	S3B
VDY585	*BY4741 ynk1Δ::KANMX*	S3C
VDY619	*BY4741 atg1Δ::ATG1(M102G) ynk1Δ::KANMX atg13Δ::URA*	S3D
VDY611	*BY4741 atg1Δ::ATG1(M102G) ynk1Δ::KANMX*	S3D
VDY1086	*BY4741 atg1Δ::ATG1(M102G) ynk1Δ::KANMX atg13Δ::ATG13-8SA ATG9-3×-FLAG::NAT atg23Δ::URA*	S3E
VDY989	*BY4741 atg1Δ::ATG1(M102G) ynk1Δ::KANMX atg13Δ::ATG13-8SA ATG6-3×-FLAG::NAT atg14Δ::URA*	S3E
VDY2420	*BY4741 atg11Δ::NAT::pTDH3-6×-FLAG-GFP-ATG11*	S4A
VDY2421	*BY4741 atg11Δ::NAT::pTDH3-6×-FLAG-GFP-ATG11ΔRBD::HIS*	S4A
VDY2238	*BY4741 atg1Δ::2×-HA-ATG1(M102G) atg13Δ::ATG13-8SA atg11Δ::LEU*	S4C
VDY2218	*BY4741 atg1Δ::2×-HA-ATG1(M102G, T226A) atg13Δ::ATG13-8SA*	S4C
VDY2230	*BY4741 atg1Δ::URA ynk1Δ::KANMX atg13Δ::ATG13-8SA atg11Δ::HIS ATG19-3×-FLAG::NAT*	S4D, S4F
VDY2422	*BY4741 atg1Δ::URA ynk1Δ::KANMX atg13Δ::ATG13-8SA atg11Δ::HIS ATG19-3×-FLAG::NAT ape1Δ::LEU*	S4D, S4F
VDY2229	*BY4741 atg1Δ::URA ynk1Δ::KANMX atg13Δ::ATG13-8SA atg11Δ::HIS ATG19Δ11BD-3×-FLAG::NAT*	S4F
VDY2586	*BY4741 atg1Δ::ATG1(M102G) ynk1Δ::KANMX atg13Δ::ATG13-8SA atg11Δ::6×-FLAG-GFP-ATG11 atg19Δ::ATG19-13×-MYC::HIS*	S4J, S4K
VDY2587	*BY4741 atg1Δ::ATG1(M102G) ynk1Δ::KANMX atg13Δ::ATG13-8SA atg11Δ::6×-FLAG-GFP-ATG11 atg19Δ::ATG19ΔABD-13×-MYC::HIS*	S4J, S4K
VDY1813	*BY4741 atg1Δ::ATG1(M102G) ynk1Δ::KANMX atg13Δ::ATG13-8SA atg11Δ::6×-FLAG-GFP-ATG11 atg19Δ::URA*	S4J, S4K

Table S2. Plasmids

Plasmids	Construct	Experiment
	pRS316	2A,2B, S1C, S2A, S3B
pVD390	pRS316:ATG1	S3B
pVD391	pRS316:ATG1(M102G)	S3B
pVD395	pRS316:2×-FLAG-ATG1	2A,2B, S2A
pVD546	pRS316:2×-FLAG-ATG1(D211A)	2A,2B, S2A
pVD558	pRS316:2×-HA-ATG1	S1C
pVD594	pRS316:2×-FLAG-ATG1(T226A)	2A,2B, S2A

SUPPLEMENTAL EXPERIMENTAL PROCEDURES

Yeast cell growth and lysate preparation:

Saturated, overnight cultures were diluted 1:100 and grown for 8 hr in YPD media (1% yeast extract, 2% peptone, 2% dextrose) to mid-log phase. YP5D (1% yeast extract, 2% peptone, 5% dextrose) media was seeded with logarithmically growing cells to achieve a final OD_{600} of ~2.0-3.0 after 9-11 doublings. When indicated, cultures were treated with 0.2 μM rapamycin (LC laboratories) in 90% ethanol/10% Tween-20 for 20 min prior to cell collection. Cells were pelleted at 3,500 × *g* for 22 min, washed with distilled water and pelleted in 50 ml Falcon tubes (3,000 × *g* for 1 min). Washed cell pellets were weighed and resuspended in 1 ml lysis buffer (50 mM HEPES-KOH, pH 6.8, 150 mM KOAc, 2 mM $MgCl_2$, 1 mM $CaCl_2$, 0.2 M sorbitol) per 6 g pellet. Lysis buffer cell suspensions were frozen, drop-wise, in liquid nitrogen and the resulting frozen material was ground in the presence of cOmplete protease inhibitor cocktail (Roche) using a Retsch PM100 ball mill (large scale, 1 liter cultures) or Retsch MM400 ball mill (small scale, 25 OD_{600} units maximum). Frozen yeast lysate powder was stored at -80 centigrade.

To induce Pex1 degradation, cells were grown overnight in YPD media to OD_{600} of 0.2 before treating them for 7 hr with 500 μM 3-indoleacetic acid (auxin) (Sigma) in DMSO or mock-treating with DMSO alone.

Protein purifications:

Atg1 complexes: Frozen lysate powder (~3,000 OD_{600} units) was prepared as described for the cell-free kinase assay. After thawing in 10ml 1 × IP buffer with 1% NP-40 and 1 × phosphatase inhibitors (5 mM sodium fluoride, 62.5 mM beta-glycerophosphate, 10 mM sodium vanadate, 50

mM sodium pyrophosphate) lysates were cleared twice at 1,000 × *g* at 4 centigrade. Protein G Dynabeads (Invitrogen) were pre-equilibrated with mouse anti-FLAG antibody (Sigma) and added to clarified extract for 3 hr at 4 centigrade. Beads were collected and washed five times with 1 × IP buffer containing 1% NP-40 and 1 × phosphatase inhibitors. FLAG-Atg1 complexes were eluted on ice with 25 µl 1 mg/ml 3 × FLAG peptide (Sigma) in IP buffer containing 1% NP-40 and 1 × phosphatase inhibitors.

FLAG-GFP-Atg11: Frozen lysate powder (~9,000 OD_{600} units) was prepared from yeast cells cultured and harvested as described for the cell-free kinase assay. After thawing in 15 ml lysis buffer, lysates were cleared twice at 1,000 × *g* before ultracentrifugation at 100,000 × *g* for 30 min to remove cellular membranes. NP-40 was added to 0.075% before incubating with 1 ml anti-FLAG resin (Sigma) for 2 hr at 4 centigrade. After extensive washing in 1 × IP buffer (containing no detergent), FLAG-GFP-Atg11 was eluted on ice with 0.5 ml 1 mg/ml 3 × FLAG peptide in IP buffer. Eluates were cleared at 20,000 × *g*, aliquoted, frozen in liquid nitrogen and stored at -80 centigrade. Protein purity was evaluated by Colloidal blue staining (Invitrogen).

Atg19-FLAG-target complexes: Frozen lysate powder (~7,500 OD_{600} units) was prepared as described for the cell-free kinase assay. After thawing in 30 ml lysis buffer, lysates were cleared twice at 1,000 × *g*. Protein G Dynabeads were pre-equilibrated with mouse anti-FLAG antibody and added to clarified extract for 3 hr at 4 centigrade. After extensive washing with lysis buffer, proteins were eluted by incubation with 150 µl 1 mg/ml 3 × FLAG peptide in IP buffer for 30 min at room temperature, aliquoted, frozen in liquid nitrogen and stored at -80 centigrade. Eluates were analyzed by Colloidal blue staining (Invitrogen).

In Figure S4J, frozen lysate powder (50 OD_{600} units) was prepared as described for the cell-free kinase assay. After thawing in 0.5 ml 1 × IP buffer with 1% NP-40 and 1 × phosphatase inhibitors, lysates were cleared twice at 3,000 × *g* at 4 centigrade. Protein G Dynabeads (Invitrogen) were pre-equilibrated with mouse anti-Myc antibody (9E10, Sigma) and added to clarified extract for 2 hr at 4 centigrade. Beads were collected, washed three times in 1 × IP buffer with 1% NP-40 and 1 × phosphatase inhibitors, and boiled in sample buffer.

Alkaline phosphatase assays:

Alkaline phosphatase assays were performed as described (Noda et al., 1995). Specifically, saturated overnight cultures were diluted to 0.2 OD_{600} in 5 ml YPD media and grown for 4 hr. Cells were pelleted, washed and resuspended in 5 mL SD-N media (0.17% yeast nitrogen base, 2% glucose). Cells were starved for 4 hr, after which 1 OD_{600} unit was collected, washed, and resuspended in 1 mL cold 145 mM NaCl with 1 mM PMSF. Cells were pelleted and resuspended in ALP lysis buffer (1 M PIPES-KOH, pH 6.8, 0.5% Triton X-100, 50 mM KCl, 100 mM KOAc, 10 mM $ZnSO_4$). Cells were lysed by vortexing with glass beads three times for 1 min with 1-min ice rests in between. Lysate was clarified at 15,000 × *g* for 5 min at 4 centigrade. 50 µl lysate, 50 µl ALP lysis buffer and 400 µl substrate solution (250 mM Tris-HCl, pH 8.5, 0.4% Triton X-100, 10 mM $MgSO_4$, 10 mM $ZnSO_4$, 1.25 mM PNPP [para-nitrophenylphosphate]) were incubated at 37 centigrade for 3-15 min, which lie in the linear range of the assay. Samples were quenched with 500 µl 1 M glycine-KOH, pH 11.0 and their absorbance at 400 nm recorded and normalized by protein concentration as determined by BCA protein assay (Pierce).

Thin layer chromatography:

Extracts from wild-type and *ynk1Δ* cells were prepared as described for kinase extracts and diluted 1:10 in 1 × kinase buffer containing competitor nucleotides and radiolabeled N^6-PhEt-ATPγ^{32}P as indicated in Figure S3C. Reactions were quenched by the addition of 5 ml 5% formic acid to 2 ml of the reaction mix. Quenched reactions (0.5 ml) were spotted on a PEI cellulose F sheets (EMD Millipore) and resolved in 0.5 M KH_2PO_4, pH 3.5. After drying, the sheet was exposed to a storage phosphor screen (GE Lifesciences) and imaged using a Typhoon TRIO scanner (GE Lifesciences). Signal quantification was performed using Image Quant TL (GE Lifesciences).

Atg1 kinase assay with radiolabeled ATP:

Purified Atg1 complexes were incubated with 2 µg/µl myelin basic protein (MBP; Sigma) and ATPγ^{32}P (0.05 µCi/µl; PerkinElmer) in kinase buffer for 30 min at room temperature. Reactions were terminated by addition of SDS sample buffer, heated, and resolved by SDS-PAGE. After drying, the gel was exposed to a storage phosphor screen, and imaged using a Typhoon Trio scanner. For quantification, triplicate reactions were analyzed using ImageQuant TL (GE Life Sciences) to measure intensities of fixed-width bands following background subtraction by the rolling-ball method.

Transmission electron microscopy:

Yeast cultures were prepared for electron microscopy as described previously (Giddings et al., 2001). Briefly, cells were collected in exponential phase in YPD medium by vacuum filtration, cryofixed using a Wohlwend Compact 02 high-pressure freezer. Samples were then freeze

substituted in 0.25% glutaraldehyde and 0.1% uranyl acetate in acetone for embedding in an embedding kit (HM20, Lowicryl). 70-nm sections were poststained in uranyl acetate and lead citrate. Sections were incubated with rabbit anti-Ape1 diluted 1:1000 or 1:2000, then with 10-nm gold-conjugated anti-rabbit IgG, before imaging at 21,000 × magnification in a transmission electron microscope (FEI CM100, Phillips). Ape1 aggregates were identified for each strain, blind to genotype, as clusters of 3 or more gold particles that colocalized with round electron-dense structures approximately 150 nm in diameter. Brightness and contrast were adjusted equally for all images in Photoshop (Adobe).

Fluorescence microscopy:

Cells were grown in synthetic dropout medium to logarithmic phase, concentrated, and imaged at room temperature on a microscope (Axiovert 200M; Carl Zeiss) equipped with a Yokogawa CSU-10 spinning disk and 488 nm and 561 nm lasers (Coherent), using an oil-immersion 63 × objective (NA of 1.4). Images were acquired using a Cascade 512B EM-CCD detector (Photometrics) and the Metamorph 7.8.8 acquisition software (Molecular Devices). Each field of view was imaged as a 7 μm Z-stack with a step-size of 0.2 μm. Images were converted to maximum intensity projections in ImageJ. Images shown in Figure 2A were assembled and adjusted for brightness and contrast – equally for all images – in Photoshop (Adobe). Atg2-GFP puncta were identified stringently, using the ImageJ Analyze Particles function, as clusters of 2 or more pixels with pixel intensity greater than or equal to 2800, and examined manually to exclude any dead cells. mCherry-Ape1 puncta were defined as clusters of 3 or more pixels with pixel intensity greater than or equal to 2300, with circularity greater than or equal to 0.70, to exclude dead cells. Colocalization analysis of computationally-identified Atg2-GFP and

mCherry-Ape1 puncta was performed manually using aligned images in Photoshop. 82.5% of all Atg2-GFP puncta colocalized with mCherry-Ape1 puncta in cells expressing wild-type Atg1. Total cells were counted manually.

Mass spectrometry:

Affinity purified FLAG-Atg1 and Atg19-FLAG complexes were prepared in triplicate as described under "Protein purifications" (~3,000 OD_{600} and ~1,500 OD_{600} units, respectively, per replicate per strain genotype) for mass spectrometry analysis by the Thermo Fisher Scientific Center for Multiplexed Proteomics at Harvard Medical School. Sample processing steps included SDS-PAGE purification of proteins followed by alkylation of cysteine and in-gel trypsin digestion. Peptides were extracted from the gel and desalted followed by peptide labeling with Tandem Mass Tag 10-plex reagents (Cargnello et al., 2010). Multiplexed quantitative mass spectrometry data were collected on an Orbitrap Fusion mass spectrometer operating in a MS3 mode using synchronous precursor selection for the MS2 to MS3 fragmentation. MS/MS data were searched against a Uniprot human database (February 2014) with both the forward and reverse sequences using the SEQUEST algorithm. Further data processing steps included controlling peptide and protein level false discovery rates, assembling proteins from peptides, and protein quantification from peptides (Weekes et al., 2014). Statistical analysis was performed using a one-way ANOVA and Benjamin Hochberg corrected p values were calculated for each protein. Alpha was set to 0.01 and only proteins with more than one quantified peptide were considered when defining proteins significantly different between preparations.

Other statistical analysis:

Statistical analysis was performed using GraphPad Prism. A one-way analysis of variance (ANOVA) was calculated for each data panel with a $p < 0.05$ significance threshold. Post hoc comparisons were conducted using Tukey's test, in which adjusted p values < 0.01 were considered significant. $n \geq 3$ for all experiments.

SUPPLEMENTAL REFERENCES

Cargnello, M., Tcherkezian, J., Dorn, J.F, Huttlin, E.L., Maddox, P.S.,, Gygi, S.P., Roux, P.P. (2012). Phosphorylation of the Eukaryotic Translation Initiation Factor 4E-Transporter (4E-T) by c-Jun N-Terminal Kinase Promotes Stress-Dependent P-Body Assembly. Mol. Cell. Biol. *32,* 4572–4584.

Giddings, T., O'Toole E.T., Morphew, M., Mastronarde, D.N., McIntosh, J.R., Winey, M. (2001). Using rapid freeze and freeze-substitution for the preparation of yeast cells for electron microscopy and three-dimensional analysis. Methods Cell Biol. *67*, 27–41.

Noda, T., Matsuura, A., Wada, Y., Ohsumi, Y. (1995). Novel system for monitoring autophagy in the yeast Saccharomyces cerevisiae. Biochem. Biophys. Res. Commun. *210*, 126–132.

Weekes M.P., Tomasec, P., Huttline, E.L., Fielding, C.A., Nusinow, D., Stanton, R.J., Wang, E.C., Aicheler, R., Murrell, I., Wilkinson, G.W., et al. (2014). Quantitative temporal viromics: An approach to investigate host-pathogen interaction. Cell *157,* 1460–1472.